CHAPTER 349

Hydrodynamics of a bar in a flood channel - the Westerschelde estuary

Claire Jeuken[1]

Abstract

Several long-term current meter observations (30 days) over a complex flood shield, i.e. an estuarine bar, display major temporal and spatial variations in current asymmetry. The variations in current asymmetry indicate the presence of small-scale circulations of sediment that are induced by smaller channels that penetrate the bar. The current meter observations and depth-averaged current patterns obtained with an ADCP revealed processes of advective flow acceleration and deceleration, as well as flow convergence and divergence, over the bars in the small channels.

Introduction

Estuaries are important coastal systems, providing natural navigation channels as well as habitats for marine flora and fauna, and recreational space. The Westerschelde forms the seaward, marine part (length 60 km) of the Schelde estuary (total length 160 km) and has a well-developed system of channels and intertidal shoals (Fig. 1a). The meandering ebb channels form the main navigation channel for ocean shipping to the harbours of Antwerpen and Gent. The shorter, straight flood channels are only suitable for small ships as the landward channel-margin of the flood channels is marked by a shallow extensive bar. Moreover, the bars in the flood channels display a complex topography due the presence of migrating connecting channels, the smaller channels that penetrate the bar and connect the main ebb and flood channel. To maintain the shipping lane dredging is carried out at the deeper bars in the main ebb channels. At present approximately $8*10^6$ m^3 of sediment is dredged annually. A further deepening of the bars, to enable the passage of larger ships, is planned for the near future. A better understanding of the morphodynamics of channels and shoals and the processes over bars in tidal channels in particular, is important for the management of the estuarine system and for determining the optimal dredging strategies. Recent developments in understanding the morphodynamics of channels and shoals have resulted in the formulation of different types of models (De Vriend (1996), De Vriend and Ribberink (1996)). Bars in tidal channels are however still understudied (Dalrymple and Rhodes, 1995 for a review).

---

[1] Institute for Marine and Atmospheric Research, Utrecht University, Department of Physical Geography, PO box 80.115, 3508 TC, Utrecht, The Netherlands.
c/o Ministry of Transport and Public Works, Directorate Zealand PO box 5014, 4330 KA Middelburg, The Netherlands.

This paper discusses the hydrodynamics of a complex bar at the end of a main flood channel, based on field observations. Flow computations with a 1D-network model indicate that this bar largely determines the distribution of tidal flow between the main ebb and flood channels during the periods of maximum flow (Jeuken, submitted). Objective of this study is to identify spatial and temporal variations of the tidal flow that are important for bar morphology and sediment transport patterns over the bar. Herein two aspects of tidal flow are considered: 1) Spatial velocity gradients and 2) differences between the velocity during ebb and flood, often referred to as current asymmetry. Spatial velocity gradients largely control processes of erosion and sedimentation. In literature tidal current asymmetry is often used as a first indicator for the direction of net sediment transport (e.g. Aubrey, 1986; Dronkers, 1986; Friederichs and Aubrey, 1988; Van de Kreeke and Robaczewska, 1993; Lessa and Masselink, 1995). In most studies current asymmetry is based on the amplitude of velocity components, often derived from a harmonic analysis of the velocity record. In this study a different approach is used to quantify variations in current asymmetry.

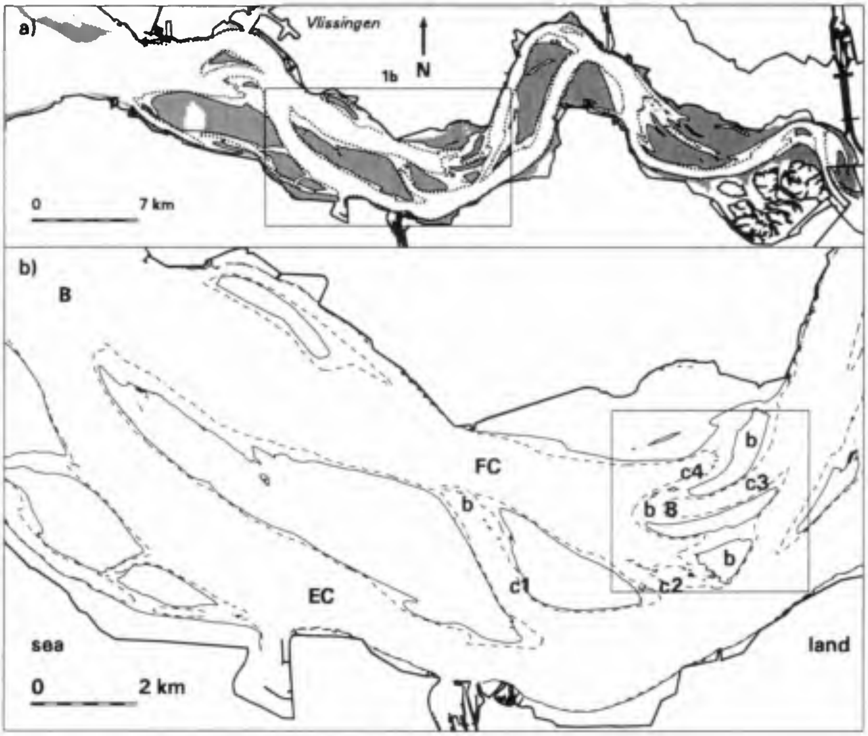

Figure 1 Location and channel configuration in the study area. a) the Westerschelde, b) the main study area. FC= main flood channel, EC=main ebb channel, c#=connecting channel (#=number), B= bar in main channel, b= bar in connecting channel.

The study area

An overview of the general hydraulic and morphologic evolution of the Schelde estuary is given by Van den Berg et.al. (in press). The main characteristics are described in this section. The Schelde is a tide-dominated meso-tidal estuary. The vertical tide displays a general asymmetry characterized by a faster rise than fall. This asymmetry increases in landward direction. In addition the vertical tide shows a pronounced neap-spring tidal variation as do the surface gradients and tidal currents. Maximum depth-averaged current velocities are in the order of 1-1.5m/s.

The larger channels in the Westerschelde display a regular returning pattern consisting of a meander-shaped ebb channel and a straight flood channel, separated by shoals (Fig. 1b). The shoals are bisected by smaller channels. These so called connecting channels form connections between the main ebb and flood channel and owe their existence to water level differences between the channels. Most connecting channels occur in the area of the bar in the main flood channel and tend to display a cyclic behaviour on the timescale of one to several decades. The shallow bar in the main flood channel is marked by various connecting channels, that originated and developed from 1986/1987. The small bars in the connecting channels are superimposed on the large bar in the main flood channel. The connecting channels C3 and C4 together reflect the morphologic characteristics of the main ebb and flood channel with respect to channel alignment and location and depth of the bars. At present (september 1996) channel C3 is rapidly degenerating. A new connecting channel has formed north of connecting channel C4.

Field observations

'Flachsee' impeller-type current meters were deployed at several locations during five measurement campaigns between April 1994 and February 1996 (Fig. 2). The current meters registered current velocity and direction for periods of thirty days with a sampling interval of ten minutes and a sampling period of one minute. At each location two current meters were deployed at the same measurement height, for validation purposes. A comparison of the double current meter deployments revealed an average difference in speed of about five percent, whereas the average difference in current direction approximated three degrees.

Detailed observations of the flow response over the small bars in two connecting channels were obtained in the summer of 1995 with a ship-borne, broad-banded two pulse Acoustic Doppler Current Profiler (ADCP). Measurements were carried out along a straight transect, oriented parallel to the general alignment of each channel, for a period of thirteen hours (Fig. 2b). The measurements along transect 1 were carried out during mean tide in June 1995. The measurements along transect 2 were obtained during spring tide in August 1995. The settings and instrumental accuracy of the ADCP during the two surveys are summarized in Table 1.

Table 1 System configuration of the ADCP during the two surveys

Transect	1	2
Acoustic frequency (kHz)	600	600
Pings per ensemble	5	20
Horizontal sampling interval (m)	10-15	40-50
Vertical bin size (m)	0.5	0.5
Depth range (m)	2.74-20	2.85-20
Velocity precision (m/s)	0.06	0.03
Compass precision (°)	1	1

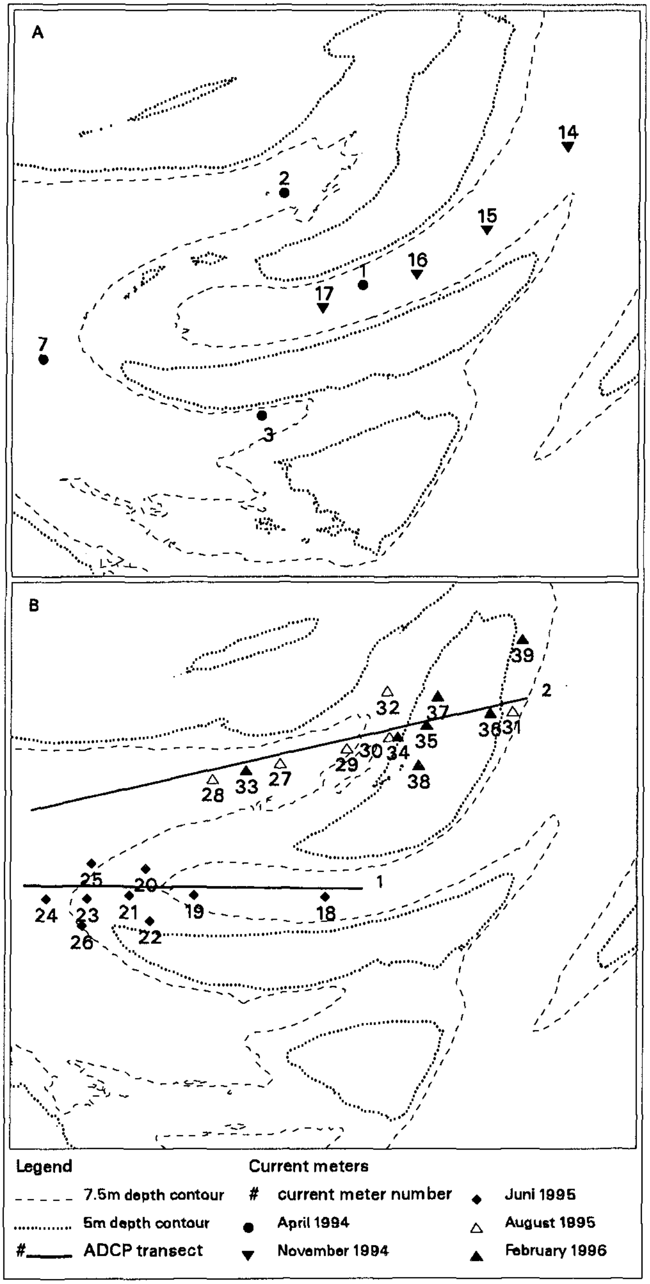

Figure 2 Locations of measurements. a) measurements in 1994 b) measurements in 1995 and 1996. For location of the bar see inset in Figure 1b.

Data-analysis

The current meter data were used to quantify temporal and spatial variations in current asymmetry and to characterize the current patterns over the small bars in the connecting channels. Prior to further analysis, the noise in the velocity data was reduced by applying a low-pass smoothing filter to the North-South and East-West velocity components.

The relative height of the current meters changed with time as a result of the large tidal range (3.3-4.75m) and the small water depths (5-13m). This variation in measurement height inhibit a comparison of measured ebb and flood velocities. Therefore measured current velocities (not direction) were converted to depth-averaged values, by assuming the logarithmic velocity profile of steady and uniform flow and an averaged roughness length based on bedform dimensions (z_0=0.033k_s, k_s=0.4m). In areas of major advective flow acceleration and deceleration this results in under-estimated (flow deceleration) and over-estimated (accelerating flow) depth-averaged velocities. These effects were not taken into account. The obtained time-series of the depth-averaged velocity vectors were then used to compute significant current vectors for each ebb and flood period. The significant velocity is defined as the mean of the 1/3 highest current velocities and represents the conditions near maximum flow over a period of about two hours. For each current meter location relationships between significant velocity (ebb and flood) and observed tidal range were determined by applying a linear regression analysis. The linear relationships were then used to compute significant ebb and flood velocities during mean, neap and spring tide. This was done by substituting the tidal range for neap, mean and spring tide in the linear relationships. Current asymmetry was then defined as the natural logarithm of the ratio of significant ebb velocity over significant flood velocity. A positive current asymmetry indicates ebb-dominated flow. A negative asymmetry indicates flood-dominated flow. The advantage of the significant velocity is, that it gives a better weighting of the tidal variation of current velocities than the often used maximum velocity.

The ADCP observations were used to determine variations in the depth-averaged flow patterns over the small bars in the connecting channels. Prior to further analysis the noise in the ADCP data was reduced by applying a low-pass, infinite impulse response filter to the North-South and East-West velocity components (Stanley et.al. 1984).

The computation of depth-averaged velocities implies extrapolation of the velocity profiles towards bottom and water surface. Extrapolation of the velocity profile was done by fitting a series of three shapefunctions through the data using a least squares method. This method has been derived from the shapefunetion approach described by Zitman (1992) and has been previously applied by Van de Meene (1994). As winds were low during the ADCP measurements, the contribution of wind stress to the current velocity was neglected. Then the vertical velocity profile in North-South and East-West direction can be expressed as (Zitman, 1992):

$$u(\zeta) = \sum_{k=1}^{m} F_k \cdot f_k(\zeta) \qquad (1)$$

where f_k is the series of shapefunctions, ζ is the dimensionless vertical coordinate and m is the number of shapefunctions (m=3 in the present analysis). The weights F_k are the unknowns to be determined using the measured velocity profile $u(\zeta)$. Figure 3 shows the applied shapefunctions together with an example of a curve fitted through observations. The shapefunction approach was used only as a statistical, curve-fitting tool, essentially to compute the depth-averaged current vectors in an objective way. The advantage of this approach is that it is possible to describe velocity profiles that deviate from e.g. a parabolic profile.

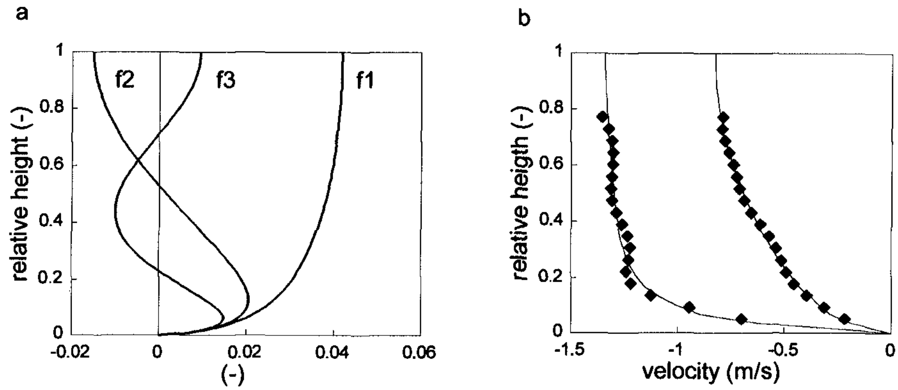

Figure 3 Shapefunction approach. a) the three shapefunctions used in the analysis, b) comparison of measured velocity components (♦) and fit (-).

Variations of current asymmetry over the bar in the main flood channel

Figure 4 shows spatial patterns of current asymmetry over the bar in the main flood channel for mean, neap and spring tide. The spatial variation of current asymmetry in Figure 4a is related to the presence and morphology of the connecting channels. In the connecting ebb channel and at the landward side of the bar in the connecting flood channel current asymmetry ranges between 0 and 0.11, indicating that ebb velocities exceed flood velocities by about 0 to 12 percent. In the connecting flood channels and at the seaward side of the bar in the connecting ebb channel, negative current asymmetries of -0.12 to -0.31 occur, indicating flood-dominated flow. In these areas flood velocities are 12 to 40 percent stronger than the ebb velocities. The bars in the connecting channels form the transition zones between ebb-dominated and flood-dominated flow. Current asymmetry changes with tidal range (Fig.4b). In the connecting ebb channel and at the landward side of the bar in the connecting flood channel, current asymmetry decreases with 6 to 25 percent when tidal range increases from 3.3 to 4.75m. At some locations in the connecting ebb channel tidal flow becomes even slightly flood-dominated during spring tide (locations 15, 20, 21 and 22 in Fig. 2). In the connecting flood channels and at the seaward side of the bar in the connecting ebb channel current asymmetry increases with 10 to 34 percent with increasing tidal range.

The spatial variation in current asymmetry indicates small-scale circulations of net sediment transport over the bar in the main flood channel, that are induced by connecting ebb and flood channels (Fig. 5a). This means net ebb transports in the ebb channel and net flood transports in the flood channel. The circulations confirm the concept of mutually evasive ebb and flood channels of Van Veen (1950), who identified the presence of ebb-dominated and flood-dominated channels on the basis of net water transports and the location of the bars in tidal channels. The changes in current asymmetry with tidal range, has two important implications for the small-scale circulations (Fig. 5b): 1) The intensity of the circulation is not constant in time and 2) the circulation is not closed. The changes in current asymmetry over the neap-spring tidal cycle indicate that the magnitude of net sediment transport, the intensity,

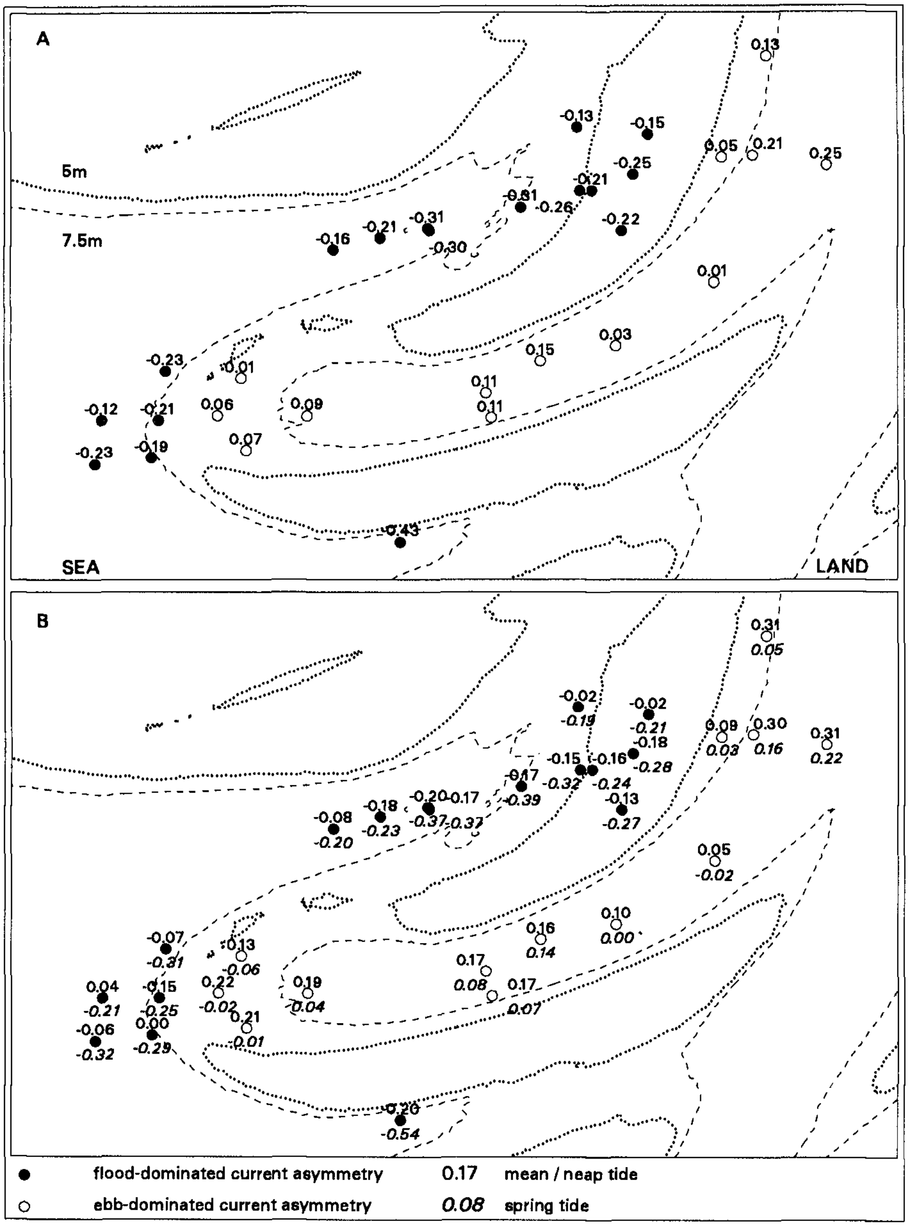

Figure 4 Patterns of current asymmetry. a) mean tide, b) neap and spring tide

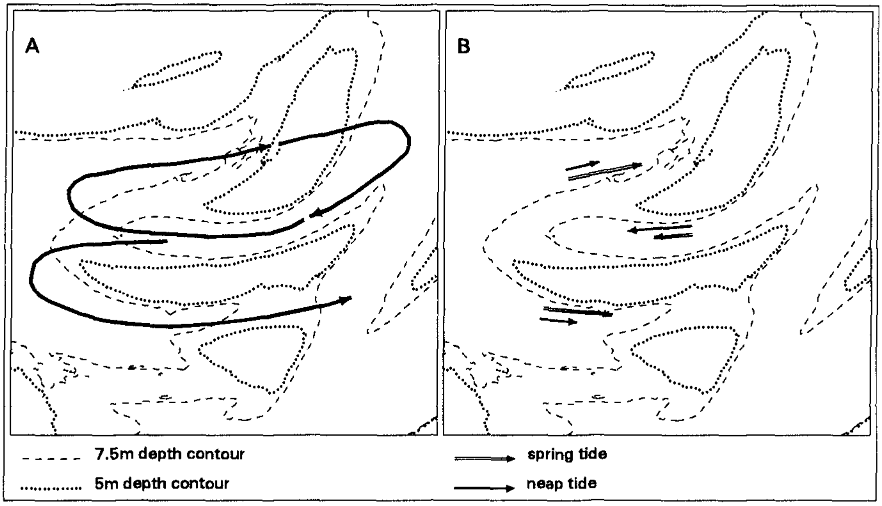

Fig. 5 Implications of the variations in current asymmetry for the patterns of net sediment transport. a) Small-scale circulations, b) the relative magnitude of net sediment transports during ncap and spring tide

changes with tidal range. The decrease in current asymmetry in the ebb channel with increasing tidal range indicates larger net ebb transports in the ebb channel during neap tide than during spring tide. The increase of current asymmetry in the flood channel indicates smaller net flood transports during neap tide than during spring tide. This difference between ebb and flood channel means that the circulation is not closed. A net flood-dominated component that increases with tidal range is likely as the flood-dominated current asymmetry is larger than the ebb-dominated current asymmetry. Moreover the morphology of the bar is dominated by connecting flood channels. Computed sediment transports (not shown), based on the current observations, confirm the above inferred spatial and temporal variations in net sediment transport.

Flow response over the bars in two connecting channels

Figure 6 and 7 summarize the flow characteristics over the bar in the connecting ebb channel during mean tidal conditions. Figure 6 shows the pattern of significant current vectors in June 1995. Figure 7 displays the pattern of depth-averaged along-transect and cross-transect velocities during accelerating, maximum and deeelerating tidal flow. During ebb the pattern of significant current vectors displays an ebb flow flowing around the bar (Fig. 6a). At the upstream side of the bar the ebb flow diverges and shows minor flow decelerations towards the bar of about 7 percent (0.08m/s). Significant current directions at location 20 and 22 differ by twenty degrees (see Fig. 2b for locations). At the downstream side of the bar the ebb flow converges and strongly decelerates with about 25 percent (0.25m/s). The ADCP observations confirm the patterns of flow deceleration (Fig. 7). The depth-averaged velocity pattern shows an instantaneous drop in current velocity as soon as the ebb flow passes the top of the bar. The depth-averaged velocity reduces with 28 percent (0.3m/s) on average. The flow reduction tends to increase with time and decreasing water level. In addition the ADCP observations show a tendency towards small flow acceleration just before the top of the bar during maximum and decelerating ebb flow. The small cross-channel velocity component, both during ebb and flood, indicates tidal flow approximately parallel to the ADCP-transect (with 5°). Thus the ebb flow diverges and decelerates towards the bar, slightly accelerates near the top of the bar and converges and strongly decelerates after passing the top of the bar.

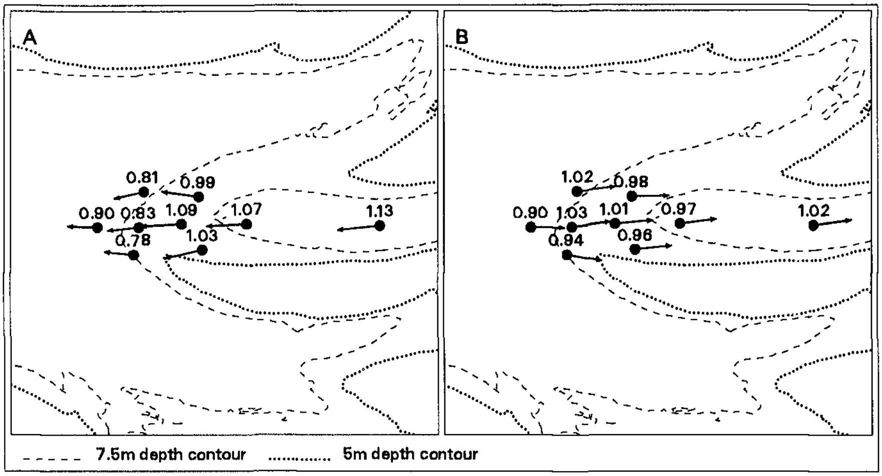

Fig. 6 Mean significant current vectors over the bar in the connecting ebb channel during mean tide in June 1995. a) ebb, b) flood.

The flood displays a small tendency towards flow around the bar (Fig. 6b). The pattern of significant current vectors shows flow divergence at the upstream (seaward) side of the bar that is accompanied by an increase in current velocities of about 14 percent (0.13m/s). At the downstream side of the bar the current vectors are aligned more or less parallel and only minor velocity gradients are observed. The ADCP observations also display flow acceleration at the upstream side of the bar (Fig.7). Depth-averaged velocities increase with about 10 percent (0.1m/s). At the downstream side, between 500 and 1200 meters, reductions in current velocity of about 10 percent (0.1m/s) are observed. Thus the flood flow slightly diverges and accelerates and decelerates over the bar.

The characteristics of the flow pattern over the bar in the connecting flood channel during spring tide, measured in August 1995 and February 1996, are summarized in Figures 8 and 9. During ebb the significant current pattern displays flow deceleration over the bar (Fig 8a). At the downstream side of the bar current velocities are 15 to 30 percent smaller than near the top of the bar (location 36, Fig. 2b). The gradual change in current direction between locations 37 and 38 of fourteen degrees, indicates a tendency towards flow convergence. The ADCP observations (Fig.9) reveal deflection of the ebb flow at the upstream side of the bar, where the current vectors are inclined towards the ADCP-transect by 15-25 degrees (not shown). Despite this current deflection a major velocity gradient over the bar can be identified. On average current velocities at the top of the bar exceed currents at the upstream and downstream side of the bar by 30 percent (0.4-0.5m/s). These large velocity differences indicate flow acceleration at the upstream side of the bar and

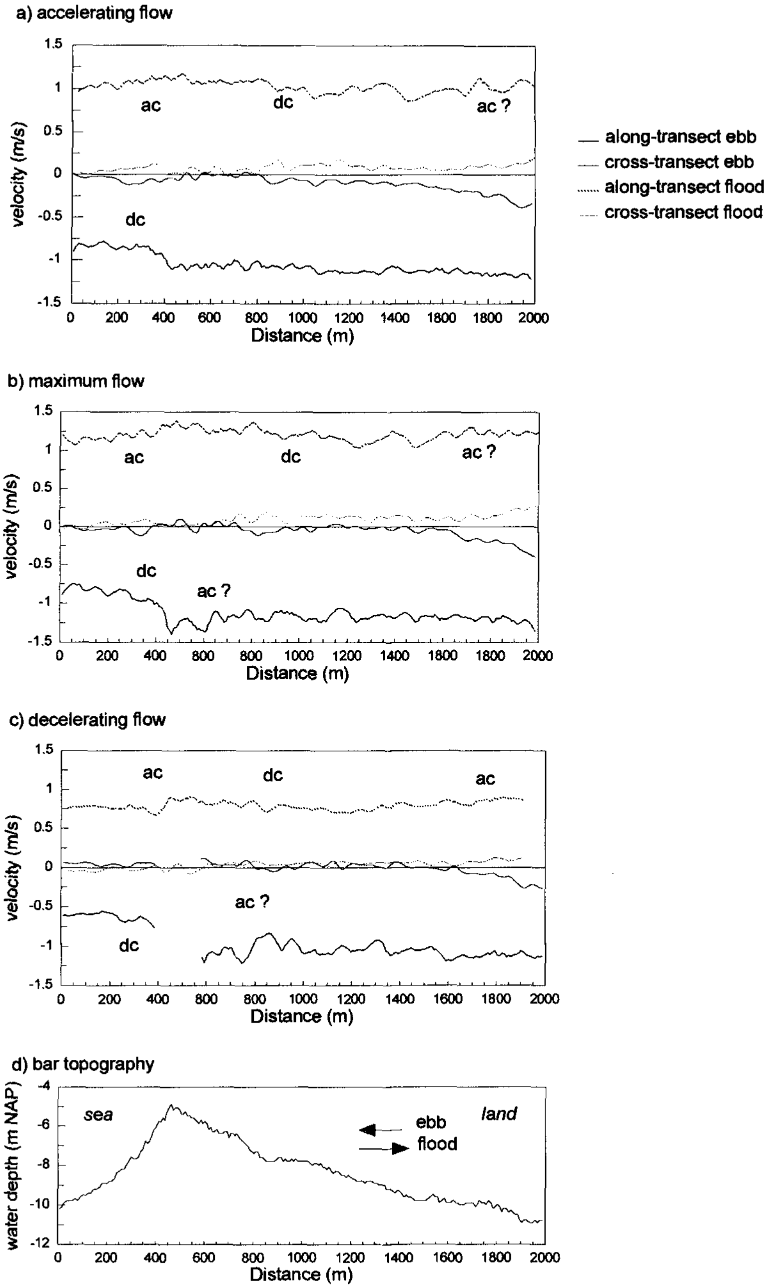

Figure 7 Depth-averaged along-transect and cross-transect velocity over the bar in the connecting ebb channel during ebb and flood on 29 June 1995. Ebb is negative, flood is positive, ac=acceleration, dc=deceleration.

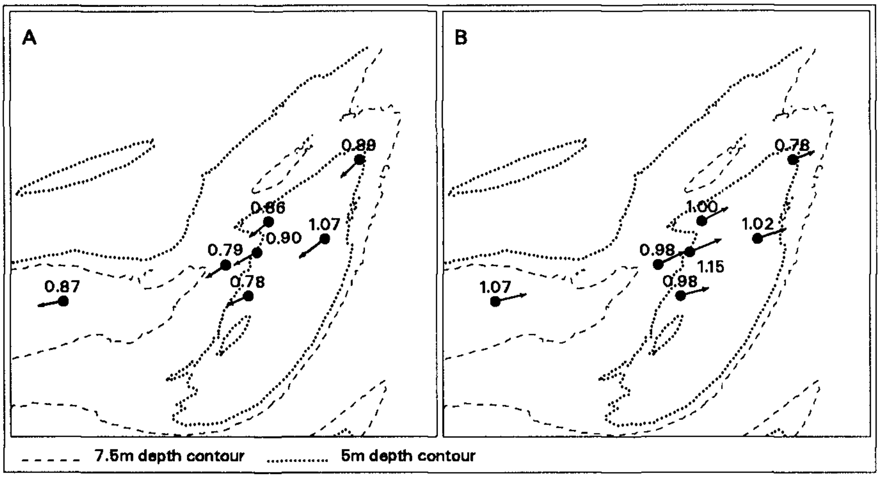

Figure 8 Mean significant current vectors over the bar in the connecting flood channel during spring tide in February 1996. a) ebb, b) flood.

flow deceleration at the downstream side of the bar. Thus the ebb flow accelerates towards the top of the bar and decelerates and converges at the downstream side of the bar. During flood the significant current vectors show a flow acceleration of about 17 percent (0.17m/s) at the upstream side of the bar (Fig. 8b). Significant current directions gradually change with twelve degrees between locations 37 and 38 (see Fig. 2b for locations), indicating minor flow divergence. The current velocity at the upstream side of the bar is 12 to 22 percent (0.13-0.22m/s) stronger than at the downstream side of the bar. This means that the flood flow decelerates over the bar. The ADCP observations show a flow deceleration of about 20 percent just before the bar (between 1700 and 2200m, Fig.9), where the flood flow diverges (not shown). At the upstream side of the bar the flood flow accelerates with about 30 percent (0.3-0.4m/s). At the downstream side flow decelerations of 40 to 50 percent (0.5-0.7m/s) are observed. The cross-transect velocity components indicate that the flood flow is less deflected by the topography of the bar than the ebb flow (inclination of 6-12° with respect to the ADCP-transect, not shown). Thus the flood flow diverges and decelerates towards the bar, accelerates near the top of the bar and strongly decelerates after passing the top of the bar.

The ADCP observations are marked by second-order fluctuations. The amplitude and length scale of these fluctuations increase with time and decreasing water level. The unfiltered velocity data display similar fluctuations. The cause of the fluctuations is not clear. Both turbulence and depth variations may cause such fluctuations.

The pronounced topography of the small bars in the connecting channels is reflected in the hydrodynamics: 1) The bars in these channels demarcate the transition zones between ebb-dominated and flood-dominated flow, 2) Neap-spring tidal variations in current asymmetry change over the bar and 3) The ebb and flood flow tend to flow around the bars of the channels and display non-uniform velocity patterns. In the connecting ebb channel largest velocity gradients are observed during ebb. In the connecting flood channel largest velocities and velocity gradients tend to occur during flood. Fluid continuity across the bar may explain the observed flow

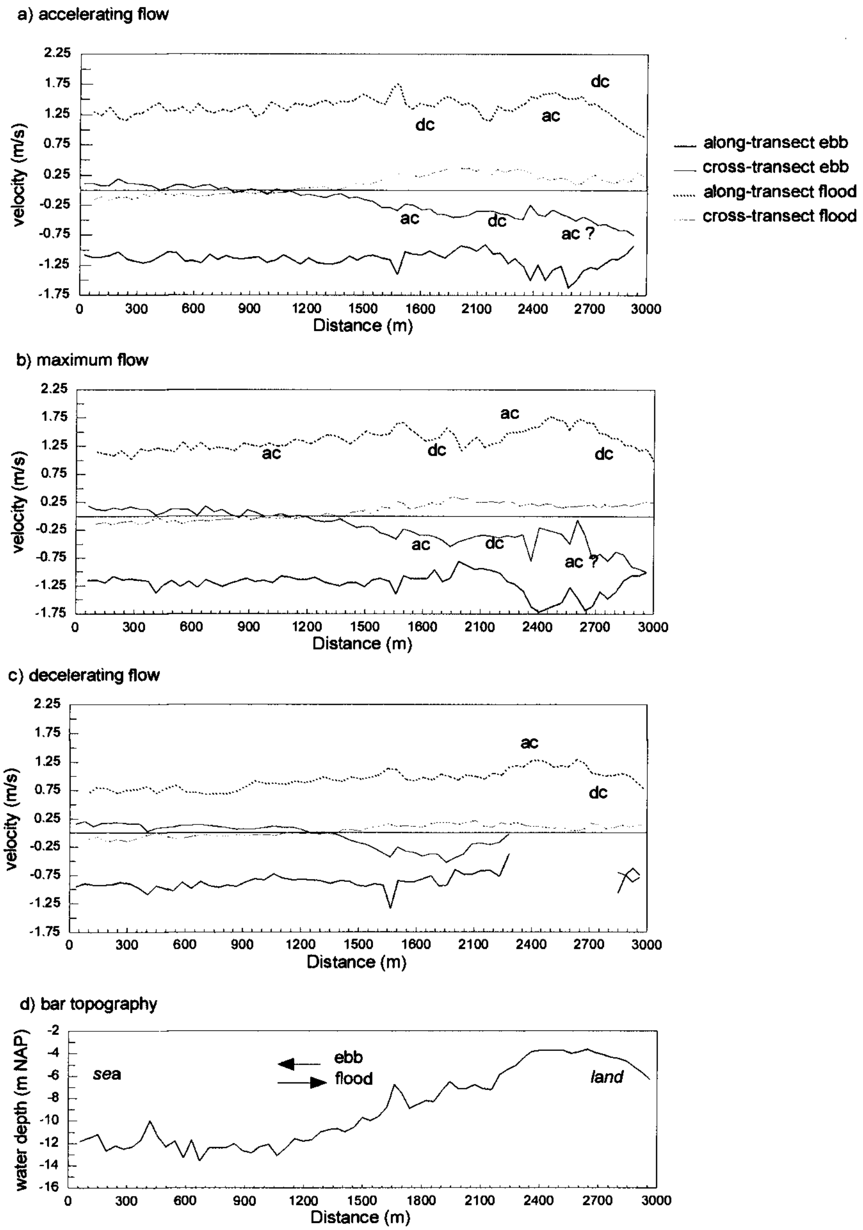

Figure 9 Depth-averaged along-transect and cross-transect velocity over the bar in the connecting flood channel during ebb and flood on 30 August 1995. Ebb is negative, flood is positive, ac=acceleration, dc=deceleration.

around the bars. Fluid continuity implies that the discharge Q (m^3/s) does not change much across the bar. The overall discharge Q is defined as $Q=b.\bar{u}.h$, where b is the width of the imaginary stream tube (m), $\bar{u}$ is the depth-averaged current velocity and h is the water depth. The changes in channel depth over the bar may result in changes in the width of the stream tube and the depth-averaged velocity. At the upstream side of the bars the flow diverges. The width of the stream tube increases. At the downstream side the flow converges. The width of the stream tube decreases. In addition to these changes in width the depth-averaged velocity increases and decreases across the bars, whereas the water depth increases and decreases. The flow over the bars shows a tendency towards flow deceleration and accelerations at the upstream side of the bar and deceleration at the downstream side. The pattern reverses every tidal phase. The implications of these flow phenomena for sediment transports, the patterns of erosion and sedimentation and the net effect over e.g. one semi-diurnal period are not evident. The implications depend on the magnitude and duration of flow accelerations and decelerations, as well as the effect of variations in stream tube width and water depth, differences in current asymmetry and the dominant sediment transport mode. The small bars are stable morphological features despite the observed flow accelerations and decelerations. This indicates that relaxation of the suspended transport may be important for the maintenance of the estuarine bars.

Conclusions

Variations of the tidal flow over the bar in the main flood channel are strongly determined by connecting channels:

1) Spatial variations in current asymmetry indicate the presence of small-scale net circulations of tidal flow and sediment transports over the bar, that are induced by connecting ebb and flood channels.
2) The changes in current asymmetry with tidal range indicate that the intensity of the circulations is not constant and that the circulations are not closed.

The flow over the small bars in the connecting channels is non-uniform and displays tendencies towards divergence, decelerations and accelerations of the flow at the upstream side of the bar and convergence and deceleration of the flow at the downstream side of the bar. The implications of the flow patterns for sediment transports and the maintenance of the bars are not evident and will be further elaborated on the basis of computations with a mathematical model and morphological analysis.

Acknowledgements

This study was funded by Directorate Zealand of the Ministry of Transport Public Works and Water Management. The measurements were carried out by the survey department of Directorate Zealand. Ir A. Langerak, drs A. Van Kleef and dr J.R. Van de Berg are greatly acknowledged for their useful comments.

Appendix

Aubrey, D.G. (1986). Hydrodynamic Controls on Sediment Transport in Well-mixed Bays and Estuaries. In: J. Van de Kreeke (ed.). Physics of shallow estuaries and Bays, p. 245-258.

Dalrymple, R.W. and R.N. Rhodes (1995). In: G.M.E. Perillo (ed.), Estuarine dunes and bars. Geomorphology and Sedimentology of Estuaries. Developments in Sedimentology 53, p. 359-422.

De Vriend, H.J. (1996). Mathematical Modelling of meso-tidal barrier island coasts. Part 1: empirical and semi-empirical models. ln: P.L.F. Liu (ed.), Advances in coastal and ocean engineering (2), p.115-149.

De Vriend, J. and J.S. Ribberink (1996) Mathematical Modelling of meso-tidal barrier island coasts. Part 11: process-based simulation models. In: P.L.F. Liu (ed.), Advances in coastal and ocean engineering (2), p.151-197

Dronkers, J. (1986). Tidal asymmetry and estuarine morphology. Neth. Jour. of Sea Res. 20 (2/3), p. 117-131.

Friederichs C.T. and D. Aubrey (1988). Non-linear Tidal Distortion in Shallow Well-mixed Estuaries: a Synthesis. Est. Coast. and Shelf Sci.(27), p. 521-545.

Jeuken, M.C.J.L. (submitted for review). Morphodynamics of connecting channels in the Westerschelde estuary (the Netherlands). Proc. Conf. Physics of Estuaries and Coastal Seas, The Hague, 1996.

Lessa, G. and G. Masselink (1995). Morphodynamic evolution of a macro-tidal barrier island. Marine Geology 129: 25-46.

Stanley, D.W., G.R. Dougherty and R. Dougherty (1984). Digital Signal Processing, Prentice Hall, 514 p.

Van de Kreeke, J. and K. Robaczewska (1993). Tide-induced residual transport on coarse sediment: application to the Ems estuary. Neth. Jour. of Sea Res. 31 (3), p.209-220.

Van de Meene, J.W.H. (1994). The shoreface-connected ridges along the central Dutch coast, Ph.D. thesis, IMAU, Utrecht Univ., Neth. Geogr. Studies 174, KNAG, Utrecht, 256 p.

Van den Berg, J.H., M.C.J.L. Jeuken and A. F. van der Spek (in press). Hydraulic processes affecting the morphology and evolution of the Westerschelde estuary. In: K.F. Nordstrom and C.J. Roman (eds.). Estuarine Shores: Evolution, Environments and Human Alterations.

Van Veen, J. (1950). Eb- en vloedscharen in de Nederlandse getijwateren. Tijdschr. Kon. Ned. Aardr. Gen. 67, p. 303-335 (in Dutch).

Zitman, T.J. (1992). Quasi three dimensional current modelling based on a modified version of Davies' shapefunction approach. Cont. Shelf Res., 12(1), p. 143-158.